Proceedings of the EuroGNC 2013, 2nd CEAS Specialist Conference
on Guidance, Navigation & Control, Delft University of Technology,
Delft, The Netherlands, April 10-12, 2013

Single vs. Two-Loop Integrated Guidance Systems

Shaul Gutman*, Tal Shima†, Sergey Rubinsky*, and Maital Levy†
Technion, Israel Institute of Technology

Abstract

Conventionally, a guidance system is formed of two loops - an autopilot that controls the rigid body with respect to the center of mass, and a guidance law that controls the center of mass toward the target. The present paper discusses the possibility of integrating these two loops into a single loop. In particular, in the class of optimal guidance laws, the absence of a state running cost term, may render some of the physical states out of bound. The presence of an autopilot assures a well behavior.

1 Introduction

A conventional guidance system consists of three main parts. The first is the (open loop) vehicle dynamics; namely, equations of motion that describe the influence of the actuator on the acceleration. The second is the closed loop dynamics based on an autopilot. The third is the guidance law. In the so called "separated" configuration the guidance law is commonly designed using a low (zero or first) order approximation of the autopilot, and acceleration is commanded (and indirectly the actuator). Recently [1-6], to name a few, a configuration, called "integrated", or "full state", has attracted the attention of the guidance community. This configuration is split into two sub-configurations. The first consists of a single feedback loop that accounts for both control and guidance, without a definite autopilot, where the guidance law commands the actuator directly. The second consists of two loops, one is the autopilot and the second is the guidance law. Based on Monte Carlo simulation results, it was claimed that as far as miss-distance is concerned, a full state (integrated) single loop system is superior to a separated guidance system. A notable exception is [4] where an integrated (full state) two-loop design is discussed.

The difference between the integrated and separated two loop designs is in the information provided to the guidance law; where in the separated design

*Department of Mechanical Engineering
†Department of Aerospace Engineering

the guidance law uses a low order approximation of the autopilot and commonly uses only information on the kinematical states (sometimes also information on states such as the missile's acceleration), while in the integrated design missile no such approximation is performed and the dynamic states are also fed back to the guidance law. In a recent paper [7] we study the three architectures discussed above, namely: Integrated (full state) single-loop, integrated (full state) two-loop, and separated two-loop [7]. Using the notion of Pareto fronts it is shown that, for a linear quadratic formulation of the interception problem, the integrated approaches are superior to the separated design. Moreover, the single and two loop integrated (full state) approaches yield identical results.

These results raise the question regarding the need of the autopilot loop. It should be emphasized that the main contributors to miss-distance are missile saturation, sensor noise, and target maneuvers. Note, that close to termination, actuators saturate. Thus, if the transfer function from the actuator to the acceleration (normal to LOS) has small damping ratio or is unstable, the attitude angle may grow dramatically, and the missile tumbles. In order to avoid such a behavior a restriction must be placed on the acceleration. This can be done in the linear quadratic approach by a running state cost term which, on the one hand, complicates the guidance law, and on the other hand, overlooks the saturation, as explained above. An alternative approach is the inverse map acceleration limiting function [2]. However, in all such approaches it is impossible to assure a guaranteed miss-distance that is so important in a preliminary design process to avoid unnecessary Monte Carlo simulations.

The present paper argues that the full state two-loop guidance scheme, based on a carefully designed autopilot, together with a nonlinear differential game based guidance law, has important advantages over full state single loop scheme. First, an autopilot is constructed. Since we are using a bounded control guidance law [8-9], the acceleration command is bounded. Since the autopilot is asymptotic stable, the actuator state is bounded by a Bounded Input Bounded Output (BIBO) argument, and easily calculated using convolution [10]. Thus, in addition to the autopilot gains, the bounds on the acceleration command and the actuator state become design parameters, in such a way that the actuator never saturates. Moreover, the bounded control guidance law, enables one to compute the guaranteed miss-distance in the presence of sensor noise and target maneuvers [11], without performing Monte Carlo simulations. This is done with the aid of a second order observer. Finally, it is worth noting that applying a nonlinear differential game based guidance law in an integrated single-loop scheme, with unstable transfer function from the actuator to the acceleration, may render a small miss-distance but a non-acceptable large attitude angle. In what follows we present three guidance laws that do not have a state running cost. As a result the guidance laws are in closed form and easy to implement. Finally, we discuss the important role of the autopilot.

2 Linear-Quadratic $\mathcal{L}^2$-Guidance

Let us open with a class of linear quadratic optimization with no running state cost term. The importance of this class lies in its closed form solution. This enables one to apply guidance laws suitable for real time implementation. In particular, consider

$$\dot{\mathbf{x}} = \mathbf{A}\mathbf{x} + \mathbf{B}\mathbf{u} \tag{1}$$

$$J = \mathbf{x}'(t_f)\ \mathbf{Q}_f\ \mathbf{x}(t_f) + \int_0^{t_f} \mathbf{u}'\mathbf{R}\ \mathbf{u}\ dt \tag{2}$$

where $\mathbf{x}\in\mathcal{R}^n$ is the state vector, $\mathbf{u} \in \mathcal{R}^m$ is the unconstrained input (control) vector, $\mathbf{A} \in\mathcal{R}^{n\times n}, \mathbf{B} \in\mathcal{R}^{n\times m}, \mathbf{Q}_f \in \mathcal{R}^{n\times n}, \mathbf{R} \in\mathcal{R}^{m\times m}$, are constant matrices, and t_f is a final (terminal) prescribed time. The control vector $\mathbf{u}$ seeks the minimization of the cost J. The terminal part of the cost, with $\mathbf{Q}_f = \mathbf{M}'\mathbf{M}$ positive definite, serves as a miss distance measure, while the integral part, with $\mathbf{R}$ positive definite, forces a finite control value.

The optimal control is known to be

$$\mathbf{u}^* = -\mathbf{R}^{-1}\mathbf{B}'\mathbf{P}(t)\mathbf{x} \tag{3}$$

where the symmetric matrix $\mathbf{P} \in\mathcal{R}^{n\times n}$ satisfies the matrix Riccati equation

$$-\dot{\mathbf{P}} = \mathbf{P}\mathbf{A} + \mathbf{A}'\mathbf{P} - \mathbf{P}\mathbf{B}\mathbf{R}^{-1}\mathbf{B}'\mathbf{P}\ ,\ \ \mathbf{P}(t_f) = \mathbf{Q}_f\ . \tag{4}$$

To calculate $\mathbf{u}^*$ explicitly, and in particular matrix $\mathbf{P}$, define the Zero-Effort-Miss (ZEM) variable

$$\mathbf{y} = \mathbf{M}\mathbf{\Phi}(t_f, t)\mathbf{x}, \tag{5}$$

where $\mathbf{\Phi}(\cdot)$ is the transition matrix of $\mathbf{A}$, satisfying

$$\dot{\mathbf{\Phi}}(t_f, t) = -\mathbf{\Phi}(t_f, t)\mathbf{A}\ \ ,\ \ \mathbf{\Phi}(t_f, t_f) = \mathbf{I}. \tag{6}$$

Since $\mathbf{A}$ is a constant matrix, $\mathbf{\Phi}(t_f, t) = \mathbf{\Phi}(t_f - t) = e^{\mathbf{A}(t_f - t)}$. Then, the optimization problem reduces to

$$\dot{\mathbf{y}} = \mathbf{X}(t_f, t)\mathbf{u}\ , \tag{7}$$

$$J = \|\mathbf{y}(t_f)\|^2 + \int \mathbf{u}'\mathbf{R}\ \mathbf{u}\ dt. \tag{8}$$

where

$$\mathbf{X}(t_f, t) = \mathbf{X}(t_f - t) = \mathbf{M}\mathbf{\Phi}(t_f - t)\mathbf{B} = \mathbf{M}\mathbf{e}^{\mathbf{A}(\mathbf{t_f}-\mathbf{t})}\mathbf{B} = \mathcal{L}^{-1}\left\{\mathbf{M}(s\mathbf{I} - \mathbf{A})^{-1}\mathbf{B}\right\}. \tag{9}$$

Note that in the **y**-space, the optimal control takes the form

$$\mathbf{u}^* = -\mathbf{R}^{-1}\mathbf{X}'(t_{go})\ \mathcal{P}\ \mathbf{y}$$

where the matrix Riccati differential equation $\mathcal{P}$ satisfies

$$-\dot{\mathcal{P}} = -\mathcal{P}\mathbf{X}\mathbf{R}^{-1}\mathbf{X}'\mathcal{P}, \quad \mathcal{P}(t_f) = \mathbf{I}. \tag{10}$$

Note that if $\mathbf{M} \in \mathcal{R}^{\ell\times n}$, it follows that $\mathcal{P}\in\mathcal{R}^{\ell\times\ell}$. Define the time-to-go $t_{go} = t_f - t$, with $dt_{go} = -dt$. Then,

$$\frac{d}{dt_{go}}\mathcal{P}(t_{go}) = -\mathcal{P}\mathbf{X}\mathbf{R}^{-1}\mathbf{X}'\mathcal{P}\ , \ \ \mathcal{P}(0) = \mathbf{I}. \tag{11}$$

and the solution is [12]

$$\mathcal{P}(\mathbf{t}_{go}) = \left[\mathbf{I} + \int_0^{t_{go}} \mathbf{X}(\boldsymbol{\tau})\mathbf{R}^{-1}\mathbf{X}'(\tau)d\tau\right]^{-1}. \tag{12}$$

Finally, the optimal control, becomes

$$\mathbf{u}^*(\mathbf{y}, t_{go}) = -\mathbf{R}^{-1}\mathbf{X}'(t_{go})\left[\mathbf{I} + \int_0^{t_{go}} \mathbf{X}(\boldsymbol{\tau})\mathbf{R}^{-1}\mathbf{X}'(\tau)d\tau\right]^{-1}\mathbf{y}. \tag{13}$$

Remark 1 *If* $\mathbf{R} = \mathbf{rI}$, *then* $\mathbf{u}^* = -\mathbf{X}'(t_{go})\left[r\mathbf{I} + \int_0^{t_{go}} \mathbf{X}(\boldsymbol{\tau})\mathbf{X}'(\tau)d\tau\right]^{-1}\mathbf{y}$.

3 Linear-Quadratic $\mathcal{H}^\infty-$Guidance

Consider the following dynamic equation, where compared to (1), a maximizer **v** is also present.

$$\dot{\mathbf{x}} = \mathbf{A}\mathbf{x} + \mathbf{B}\mathbf{u} + \mathbf{C}\mathbf{v} \tag{14}$$

The control **u** seeks the minimization of the cost

$$J = \mathbf{x}'(t_f)\ \mathbf{Q}_f\ \mathbf{x}(t_f) + \int_{t_0}^{t_f} \mathbf{u}'\mathbf{R}\mathbf{u}\ dt. \tag{15}$$

Assume that **u** and **v** are free, and associate with J, the auxiliary cost

$$J_1 = \mathbf{x}'(t_f)\ \mathbf{Q}_f\ \mathbf{x}(t_f) + \int_{t_0}^{t_f} [\mathbf{u}'\mathbf{R}\mathbf{u} - \mathbf{v}'\mathbf{S}\mathbf{v}]\ dt, \tag{16}$$

and find a saddle point (if it exists) with respect to the minimizer $\mathbf{u}$ and the maximizer $\mathbf{v}$.

The optimal control is known to satisfy

$$\mathbf{u}^* = -\mathbf{R}^{-1}\mathbf{B}'\mathbf{P}(t)\mathbf{x}$$

where

$$\begin{aligned} -\dot{\mathbf{P}} &= \mathbf{PA} + \mathbf{A}'\mathbf{P} - \mathbf{P}(\mathbf{BR}^{-1}\mathbf{B}' - \mathbf{CS}^{-1}\mathbf{C}')\mathbf{P}, \\ \mathbf{P}(t_f) &= \mathbf{Q}_f \ . \end{aligned} \tag{17}$$

For $\mathbf{x}_0 = 0$, one has

$$J^* \triangleq J(\mathbf{u}^*, \mathbf{v}) \leq \int_{t_0}^{t_f} \mathbf{v}'\mathbf{S}\mathbf{v} \ dt, \tag{18}$$

which is assumed to be bounded. For the special case, $\mathbf{R} = k\mathbf{I}$, and $\mathbf{S} = \rho\mathbf{I}$,

$$\mathbf{u}^* = -k^{-1}\mathbf{B}'\mathbf{P}\mathbf{x} \tag{19}$$

$$-\dot{\mathbf{P}} = \mathbf{PA} + \mathbf{A}'\mathbf{P} - \mathbf{P}\left(k^{-1}\mathbf{BB}' - \rho^{-1}\mathbf{CC}'\right)\mathbf{P} \tag{20}$$

$$\mathbf{P}(t_f) = \mathbf{Q}_f \tag{21}$$

To generate a guidance law, let $\mathbf{Q}_f = \mathbf{M}'\mathbf{M}$, and transform the state equations into the ZEM space,

$$\mathbf{y} = \mathbf{M}\mathbf{\Phi}(t_f, t)\mathbf{x}, \tag{22}$$

$$\dot{\mathbf{y}} = \mathbf{X}(t_f, t)\mathbf{u} + \mathbf{Y}(t_f, t)\mathbf{v}, \tag{23}$$

$$J = \|\mathbf{y}(t_f)\|^2 + \int (\mathbf{u}'\mathbf{R}\ \mathbf{u} - \mathbf{v}'\mathbf{S}\mathbf{v}) \ dt, \tag{24}$$

where

$$\mathbf{X}(t_f, t) = \mathcal{L}^{-1}\left\{\mathbf{M}(s\mathbf{I} - \mathbf{A})^{-1}\mathbf{B}\right\}, \ \ \mathbf{Y}(t_f, t) = \mathcal{L}^{-1}\left\{\mathbf{M}(s\mathbf{I} - \mathbf{A})^{-1}\mathbf{C}\right\} \tag{25}$$

Note that in the $\mathbf{y}$-space, the matrix Riccati differential equation is

$$-\dot{\mathcal{P}} = -\mathcal{P}(\mathbf{XR}^{-1}\mathbf{X}' - \mathbf{YS}^{-1}\mathbf{Y}')\mathcal{P}, \quad \mathcal{P}(t_f) = \mathbf{I}. \tag{26}$$

In terms of time-to-go,

$$\frac{d}{dt_{go}}\mathcal{P}(t_{go}) = -\mathcal{P}(\mathbf{XR}^{-1}\mathbf{X}' - \mathbf{YS}^{-1}\mathbf{Y}')\mathcal{P} \ , \ \ \mathcal{P}(0) = \mathbf{I}. \tag{27}$$

The solution becomes [12]

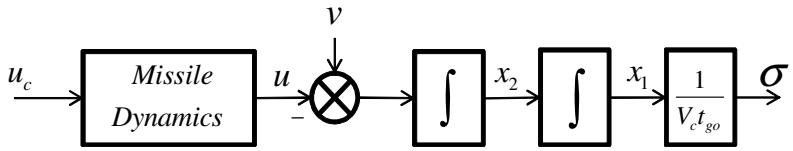

Figure 1: Open Loop Guidance Block Diagram

$$\mathcal{P}(\mathbf{t}_{go}) = \left[\mathbf{I} + \int_0^{t_{go}} (\mathbf{X}(\boldsymbol{\tau})\mathbf{R}^{-1}\mathbf{X}'(\tau) - \mathbf{Y}(\boldsymbol{\tau})\mathbf{S}^{-1}\mathbf{Y}'(\tau))(\tau)d\tau\right]^{-1}. \tag{28}$$

$$\mathbf{u}^*(\mathbf{y}, t_{go}) = -\mathbf{R}^{-1}\mathbf{X}'(t_{go})\left[\mathbf{I} + \int_0^{t_{go}} (\mathbf{X}(\boldsymbol{\tau})\mathbf{R}^{-1}\mathbf{X}'(\tau) - \mathbf{Y}(\boldsymbol{\tau})\mathbf{S}^{-1}\mathbf{Y}'(\tau))(\tau)d\tau\right]^{-1}\mathbf{y}. \tag{29}$$

4 $\mathcal{L}^2-$ SISO Guidance

Consider a standard Single-Input-Single-Output (SISO) open loop guidance block diagram as described by Figure 1. In this figure, x_1 is the target-missile separation perpendicular to the Line Of Sight (LOS), σ is the LOS orientation relative to a fixed direction, V_c is the closing speed, such that $R = V_c t_{go}$ is the range, u and v are the missile and target acceleration perpendicular to the LOS, the dynamics has $G_M(s)$ as the missile transfer function, and u_c is the missile command acceleration. Suppose $G_M(s)$ has the realization $\{\mathbf{A}_M, \mathbf{B}_M, \mathbf{c}_M, d_M\}$, with $\mathbf{z}$ as state vector. In this section, the target does not maneuver, $v = 0$. The state space equations are

$$\dot{\mathbf{x}} = \mathbf{A}\mathbf{x} + \mathbf{b}u_c \tag{30}$$

where

$$\mathbf{A} = \begin{bmatrix} 0 & 1 & 0 \\ 0 & 0 & -\mathbf{c}_M \\ 0 & 0 & \mathbf{A}_M \end{bmatrix} \qquad \mathbf{b} = \begin{bmatrix} 0 \\ -d_M \\ \mathbf{b}_M \end{bmatrix} \tag{31}$$

and the cost

$$J = |\mathbf{m}x(t_f)|^2 + \int_0^{t_f} ru_c^2 dt \tag{32}$$

where

$$\mathbf{m} = \begin{bmatrix} 1 & 0 & 0 \end{bmatrix} . \tag{33}$$

$$u_c^* = N^*(t_{go}) \left[V_c \dot{\sigma} - \frac{1}{t_{go}^2} \mathcal{L}^{-1} \{ c_M (sI - A_M)^{-1} / s^2 \} \, \mathbf{z} \right] \tag{34}$$

where

$$N^*(t_{go}) = \frac{\mathcal{L}^{-1} \left\{ G_M(s)/s^2 \right\} \, t_{go}^2}{r + \int\limits_0^{t_{go}} \left[\mathcal{L}^{-1} \left\{ G_M(s)/s^2 \right\} \right]^2 (\xi) d\xi} \tag{35}$$

5 $\mathcal{H}^\infty-$ SISO Guidance

Consider the state equation

$$\dot{\mathbf{x}} = \mathbf{A}\mathbf{x} + \mathbf{b}u_c + \mathbf{c}v \tag{36}$$

where

$$\mathbf{A} = \begin{bmatrix} 0 & 1 & 0 \\ 0 & 0 & -\mathbf{c}_M \\ 0 & 0 & \mathbf{A}_M \end{bmatrix} , \quad \mathbf{b} = \begin{bmatrix} 0 \\ -d_M \\ \mathbf{b}_M \end{bmatrix} , \quad \mathbf{c} = \begin{bmatrix} 0 \\ 1 \\ 0 \end{bmatrix} \tag{37}$$

and the cost

$$\begin{aligned} J &= |\mathbf{m}\mathbf{x}(t_f)|^2 + \int\limits_0^{t_f} (r u_c^2 - \rho v^2) dt, \\ \mathbf{m} &= \begin{bmatrix} 1 & 0 & 0 \end{bmatrix} . \end{aligned} \tag{38}$$

The optimal guidance

$$u_c^* = N^*(t_{go}) \left[V_c \dot{\sigma} - \frac{1}{t_{go}^2} \mathcal{L}^{-1} \{ c_M (sI - A_M)^{-1} / s^2 \} \, \mathbf{z} \right] \tag{39}$$

$$N^*(t_{go}) = \frac{\mathcal{L}^{-1} \left\{ G_M(s)/s^2 \right\} \, t_{go}^2}{r + \int\limits_0^{t_{go}} \left(\left[\mathcal{L}^{-1} \left\{ G_M(s)/s^2 \right\} \right]^2 - \frac{r}{\rho} \left[\mathcal{L}^{-1} \left\{ 1/s^2 \right\} \right]^2 \right) (\xi) d\xi} . \tag{40}$$

Remark 2 *The extension to a non ideal target is straightforward and is omitted here.*

6 Nonlinear Guaranteed-Miss Guidance

Consider two objects, M (missile) and T (target), move according to

$$\dot{\mathbf{x}} = \mathbf{A}\mathbf{x} + \mathbf{b}u_c + \mathbf{c}v, \tag{41}$$

where $\mathbf{x} \in \mathcal{R}^n$ is the state, $u_c \in \mathcal{R}^1$ is M's control variable, $v \in \mathcal{R}^1$ is T's control variable, and $\mathbf{A} \in \mathcal{R}^{n\times n}, \mathbf{b} \in \mathcal{R}^n, \mathbf{c} \in \mathcal{R}^n$ are defined in (37). Suppose the control variables are restricted according to

$$\begin{aligned} |u_c| &\leq \rho_u \\ |v| &\leq \rho_v. \end{aligned} \tag{42}$$

With the above dynamics we associate a terminal cost,

$$J = |\mathbf{m}\mathbf{x}(t_f)|, \tag{43}$$

where $\mathbf{m} \in \mathcal{R}^{1\times n}$ is a *constant* row vector, and t_f is the final time. We assume that M is the minimizer (of J) while T is the maximizer. We say that $\{u_c^*, v^*\}$ is an optimal pair, if it satisfies the saddle point inequality

$$J(u_c^*, v) \leq J(u_c^*, v^*) \triangleq J^* \leq J(u_c, v^*), \tag{44}$$

where J^* is the saddle point value. To find a saddle point, we first transform the state vector $\mathbf{x}$ into the so called *zero-effort-miss* variable y

$$y = \mathbf{m}\mathbf{\Phi}(t_f, t)\mathbf{x}. \tag{45}$$

Note that in this paper $\mathbf{d}$ is a row vector. Thus, y is a scalar. Differentiating (13), we have

$$\begin{aligned} \dot{y} &= Xu + Yv, \\ J &= |y(t_f)|, \\ |u| &\leq \rho_u \ , \ |v| \leq \rho_v. \end{aligned} \tag{46}$$

Where,

$$X = \mathbf{m}\mathbf{\Phi}\mathbf{b} = \mathcal{L}^{-1}\left\{\mathbf{m}(s\mathbf{I} - \mathbf{A})^{-1}\mathbf{b}\right\}, \quad Y = \mathbf{m}\mathbf{\Phi}\mathbf{c} = \mathcal{L}^{-1}\left\{\mathbf{m}(s\mathbf{I} - \mathbf{A})^{-1}\mathbf{c}\right\}. \tag{47}$$

The advantage of this representation lies in the fact that the new state space is the two dimensional (y, t)-plane. To present the saddle point strategy, we use $t_{go} = t_f - t$ as the time-to-go and pass to $(|y|, t)$-plane. Refer to Figure 2 and define

$$\alpha(\xi) = -\rho_u |X(\xi)| + \rho_v |Y(\xi)|. \tag{48}$$

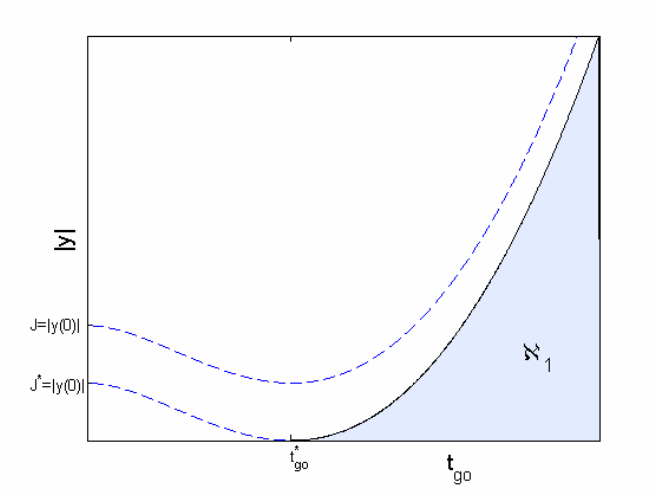

Figure 2: DG $(|y|, t_{go})$ space

Then, the saddle point value is

$$J^* = \underset{t_{go}\geq 0}{Sup}\left\{\int_0^{t_{go}} \alpha(\xi)d\xi\right\} \triangleq \int_0^{t^*_{go}} \alpha(\xi)d\xi. \tag{49}$$

The optimal trajectory is

$$|y^*(t_{go})| = |y(0)| - \int_0^{t_{go}} \alpha(\xi)d\xi, \qquad |y(0)| \geq J^*. \tag{50}$$

Define the region

$$\aleph_1 = \left\{(|y|, t_{go}) : t_{go} > t^*_{go}, \quad |y| < -\int_{t^*_{go}}^{t_{go}} \alpha(\xi)d\xi\right\}. \tag{51}$$

Then, the optimal strategy pair $\{u_c^*, v^*\}$ is given by [8-9]

$$u_c^* = \begin{cases} \text{arbitrary in } \aleph_1, \\ -\rho_u \cdot sgn(X) \cdot sgn(y) \quad \text{outside } \aleph_1, \end{cases} \tag{52}$$

$$v^* = \begin{cases} \text{arbitrary in } \aleph_1, \\ \rho_v \cdot sgn(Y) \cdot sgn(y) \quad \text{outside } \aleph_1. \end{cases} \tag{53}$$

To apply the previous results to guidance systems, consider the standard motion in the neihbohood of a collision course as depicted in Figure 1. In this figure, *the target is assumed ideal* with acceleration v perpendicular to the LOS, $G_M(s)$ is the missile transfer function, x_1 is the target-missile separation

perpendicular to the LOS, V_c is the closing speed such that the range $R = V_c t_{go}$, and σ is the LOS angle with respect to some inertial reference line. At this stage we assume that σ is noise free. It is readily seen that

$$X(s) = -G_M(s)/s^2 \ , \ \ Y(s) = 1/s^2 \ . \tag{54}$$

Let

$$G_M \triangleq \left\{\hat{\mathbf{A}}, \hat{\mathbf{b}}, \hat{\mathbf{c}}\right\}$$

be a realization of $G_M(s)$, with a state vector $\mathbf{z}$. Note that $G_M(s)$ is the control transfer function. As explained in the next section, we usually consider it as the closed loop transfer function. That is, it includes the autopilot. Thus, it is asymptotically stable, and for ideal tracking, satisfies $G_M(0) = 1$. Define the system state vector as

$$\mathbf{x} = \begin{bmatrix} x_1 \\ x_2 \\ \mathbf{z} \end{bmatrix} .$$

Then, from Figure 1, $\sigma = x_1/V_c t_{go}$. Taking the derivative yields $x_1 + t_{go} x_2 = t_{go}^2 V_c \dot{\sigma}$. Thus, the ZEM variable,

$$\begin{aligned} y &= x_1 + t_{go} x_2 - \mathcal{L}^{-1}\left\{\hat{\mathbf{c}}(s\mathbf{I} - \hat{\mathbf{A}})^{-1}/s^2\right\}\mathbf{z} \\ &= t_{go}^2\left[V_c\dot{\sigma} - \frac{1}{t_{go}^2}\mathcal{L}^{-1}\left\{\hat{\mathbf{c}}(s\mathbf{I} - \hat{\mathbf{A}})^{-1}/s^2\right\}\mathbf{z}\right]. \end{aligned} \tag{55}$$

Recall that the optimal strategy in $\aleph_1$ is arbitrary. Following [8], we *choose* in $\aleph_1$ a linear strategy. To this end, note that

$$u^* = \frac{\rho_u}{|y|_{\partial\aleph_1}}\ y.$$

Thus, the optimal strategy for the missile becomes

$$\begin{aligned} (i) \quad t_{go} &> t_{go}^* : \ u^* = \rho_u \cdot sat\left\{N^*(V_c\dot{\sigma} - \mathbf{N}_a\mathbf{z})\right\}, \\ N^* &= \frac{\rho_u \cdot t_{go}^2 \cdot sgn\left[\mathcal{L}^{-1}\left\{G_M(s)/s^2\right\}\right]}{J^* + \rho_u \int_0^{t_{go}} \left|\mathcal{L}^{-1}\left\{G_M(s)/s^2\right\}\right| d\xi - \frac{1}{2}\rho_v t_{go}^2}, \\ \mathbf{N}_a &= \frac{1}{t_{go}^2}\mathcal{L}^{-1}\left\{\hat{\mathbf{c}}(s\mathbf{I} - \hat{\mathbf{A}})^{-1}/s^2\right\}, \\ t_{go}^* : & \quad \left|\mathcal{L}^{-1}\left\{G_M(s)/s^2\right\}\right|_{t_{go}^*} - \frac{\rho_v}{\rho_u} t_{go}^* = 0, \\ (ii) \quad t_{go} &\leq t_{go}^* : \ u^* = \rho_u \cdot sgn\left\{(V_c\dot{\sigma} - \mathbf{N}_a\mathbf{z})\right\} \cdot sgn\left[\mathcal{L}^{-1}\left\{G_M(s)/s^2\right\}\right], \end{aligned} \tag{56}$$

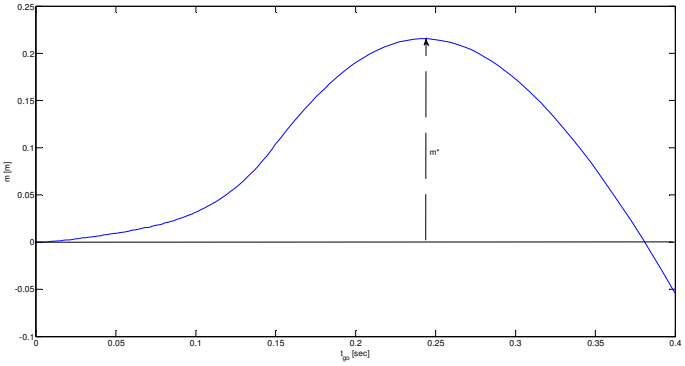

Figure 3: Typical $m(t_{go})$ function

where the saddle point value, or the guaranteed miss, has the form

$$J^* = \underset{t_{go}\geq 0}{Sup}\{m(t_{go})\} = \underset{t_{go}\geq 0}{Sup}\left\{-\rho_u \int_0^{t_{go}} \left|\mathcal{L}^{-1}\{G_M(s)/s^2\}\right| d\xi + \frac{1}{2}\rho_v t_{go}^2\right\}. \quad (57)$$

The function $m(t_{go})$ is calculated using the block diagram presented in Figure 3, where the dashed blocks are the contributions of a non ideal target. Finally a typical $m(t_{go})$ function is depicted in Figure 4.

Remark 3 *It is possible, of course, to use the strategy (56ii) everywhere.*

Finally, it is worthnoting that the above results are extended to the case of angular noise in [11], where a second order observer is used.

7 Autopilot Role

The above three guidance laws, both linear ((34)-(35) and (39)-(40)), and nonlinear ((56)-(57)), share one common property; namely, the cost does not include a state running term. As a result, these strategies are in closed form, suitable for implementation. However, the absence of a state running cost term, may result in miss-distance as required, but some important states, such as body angle, may diverge to unacceptable values. To overcome this difficulty, either an autopilot is used and a two-loop guidance results, or a state running cost term is used [3], and a single-loop guidance results as depicted in Figure 5. Note that for SISO LQ full state optimization, the single-loop and the two-loop strategies are equivalent [7]. Yet, it is known that close to termination, actuators saturate. This, of course, induces miss-distance. While linear quadratic approach does not guarantee a miss-distance value, the saturation deteriorates the miss even

further. This paper suggests that the use of a nonlinear strategy such as (56), enables the designer to avoid saturation altogether, by carefully selecting the guidance bound ρ_u, as well as the autopilot parameters. This can be done using convolutin from ρ_u to the required actuator variable [10]. Thus, the design proceedure consists of the following steps. First, given an open loop dynamics, such as the one described by Figure 6, construct a closed loop structure, called autopilot, for stability and tracking, as depicted in Figure 7. The feedback gains are subject to changes in a later step. Second, construct a two-loop guidance scheme, described by Figure 8, using a guidance law such as the nonlinear (56). A more advanced scheme, described in Figure 9, accounts for angular noise [11]. Third, perform a parameter study using the convolution in [10] and the guaranteed miss-distance (Figs. 3, 4), or the one in [11]. The parameters include the autopilot gains, the guidance bound ρ_u, the allowed actuator limit, the two observer gains, the target maneuver bound, the noise bound, and the allowed miss-distance. Fourth, if no parameter set renders the required miss, improve the missile maneuverability and repeat the parameter study. It is stressed that the above procedure is performed in an early stage of the design so as to save later design iterations. Finally note that an autopilot, carefully designed, remains stable at saturation.

References

[1] C.F. Lin, Q. Wang, J.L. Speyer, J.H. Evers, and J.R. Cloutier, "Integrated Estimation, Guidance and Control System Design using Game Theoretic Approach", Proc. American Control Conf., Evanston, IL, 1992, pp. 3220-3224.

[2] N. F. Palumbo, B. E. Reardon, and R. A. Blauwkamp, "Integrated Guidance and Control for Homing Missiles", *Johns Hopkins APL Technical Digest*, Vol. 25, No. 2, pp. 121-139, 2004.

[3] N. F. Palumbo, and T. D. Jackson, "Integrated Missile Guidance and Control: A State Dependent Riccati Differential equation Approach", *Proc. IEEE Conf. Control Applications*, Kohala Coast - Island, Hawii, 1999, pp. 243-248.

[4] Shkolnikov, I., Shtessel, Y. B. and Lianos, D., "Integrated Guidance-Control System of a Homing Interceptor: Sliding Mode Approach", AIAA, GNC Conference, August 6–9, 2001, pp. 1–11.

[5] Shima, T., Idan, M. and Golan, O. "Sliding-Mode Control for Integrated Missile Autopilot Guidance", *J. Guidance, Control, and Dynamics*, Vol. 29, No. 2, 2006, pp. 250-260.

[6] M. Idan, T. Shima, and O.M. Golan, "Integrated Sliding Mode Autopilot-Guidance for Dual-Control Missiles", *J. Guidance, Control, and Dynamics*, Vol. 30, No. 4, pp. 1081-1089, 2007.

[7] M. Levy, T. Shima, and S. Gutman, "Linear Quadratic Integrated vs Separated Autopilot-Guidance Design", Submitted to *J. Guidance, Control, and Dynamics*.

[8] S. Gutman, "On Optimal Guidance for Homing Missiles", *J. Guidance and Control*, Vol. 2, No. 4, pp.296-300, 1979.

[9] S. Gutman, *Applied Min-Max Approach to Missile Guidance and Control*, Progress in Astronautics and Aeronautics, Vol. 209, AIAA, Washington, D.C., 2005.

[10] S. Gutman, and O. Ben Aharon, "Agility vs Stability in Homing Missiles", *AIAA, GNC, CP-6433*, Keystone, Colorado, 2006.

[11] S. Gutman, O. Goldan, and S. Rubinsky, "Guaranteed Miss Distance in Guidance Systems with Bounded Controls and Bounded Noise", *J. Guidance, Control, and Dynamics*, Vol. 35, No. 3, pp. 816-823, 2012.

[12] Rusnak, I., Weiss, H., Eliav, R., and Shima, T., "Missile Guidance with Constained Terminal Body Angle," 26th IEEE Convention of Electrical and Electronics Engineers in Israel, 17-20 Nov 2010, pp. 45–49.

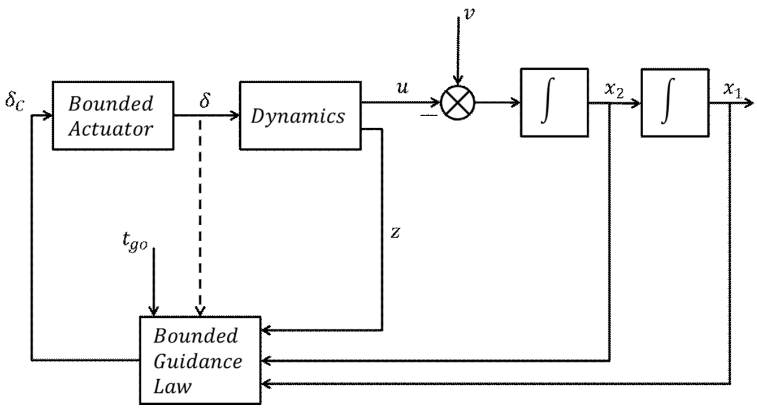

Figure 4: Integrated Single-Loop Guidance System

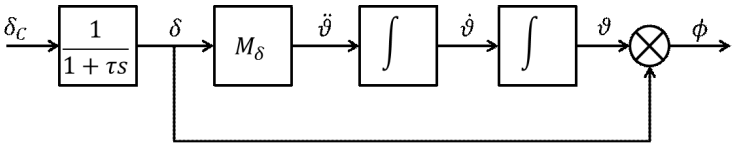

Figure 5: Unstable Open Loop Dynamics

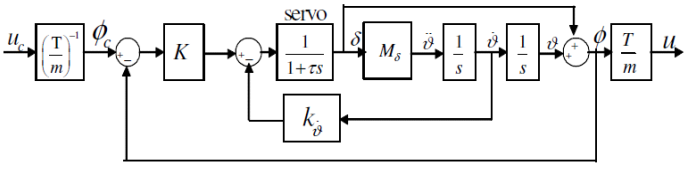

Figure 6: Stable Autopilot

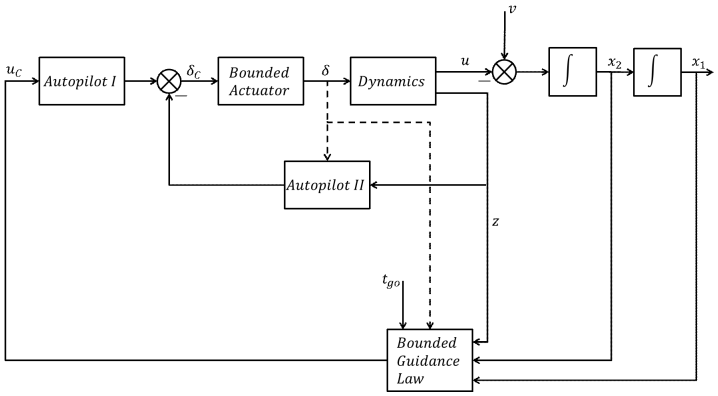

Figure 7: Integrated Two-Loop Guidance System

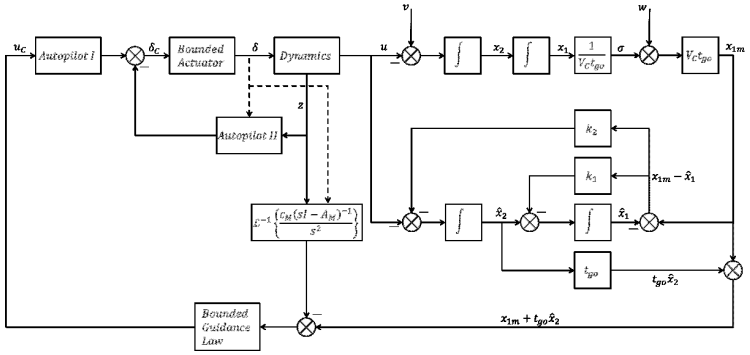

Figure 8: Integrated Two-Loop Observer Based Guidance System